Fuel-grade ethanol transport and impacts to groundwater in a pilot-scale aquifer tank

Natalie L. Cápiro[a],*, Brent P. Stafford[b], William G. Rixey[b], Philip B. Bedient[a], Pedro J.J. Alvarez[a],**

[a]Department of Civil and Environmental Engineering, Rice University, 6100 Main St.-MS 317, Houston, TX 77005, USA
[b]Department of Civil and Environmental Engineering, University of Houston, 4800 Calhoun, Houston, TX 77204-4003, USA

ARTICLE INFO

ABSTRACT

Fuel-grade ethanol (76 L of E95, 95% v/v ethanol, 5% v/v hydrocarbon mixture as a denaturant) was released at the water table in an 8150-L continuous-flow tank packed with fine-grain masonry sand. Ethanol, which is buoyant and hygroscopic, quickly migrated upwards and spread laterally in the capillary zone. Horizontal migration of ethanol occurred through a shallow thin layer with minimal vertical dispersion, and was one order of magnitude slower than the preceding bromide tracer. Dyes, one hydrophobic (Sudan-IV) and one hydrophilic (Fluorescein) provided evidence that the fuel hydrocarbons phase separated from the E95 mixture as ethanol was diluted by pore water and its cosolvent effect was diminished. Most of the added ethanol (98%) was recovered in the effluent wells that captured the flow through the high water content regions above the water table. Complementary bench-scale 2-D visualization experiments with E95 confirmed hydrocarbon phase separation, residual NAPL formation and migration within the capillary fringe. These results corroborate previous bench-scale studies showing that ethanol has high affinity for vadose-zone pore water and can migrate through the capillary zone. The pilot-scale tank experiment provides the first hydrocarbon and ethanol concentration measurements (and thus, quantification of impacts to groundwater quality) from a subsurface spill of E95 in a well-characterized system with a well-defined source. It also provides the first quantitative near-field-scale evidence that capillarity can significantly retard the vertical dispersion and horizontal advection of ethanol. Such effects could be important determinants of the extent of ethanol migration and longevity as well as groundwater impacts.

© 2006 Elsevier Ltd. All rights reserved.

1. Introduction

Ethanol is increasingly being used to meet renewable fuel requirements and to replace the oxygenate methyl tertiary-butyl ether (MTBE), which despite helping to meet Clean Air Act goals has caused widespread water contamination problems (Zogorski et al., 1996; BRP, 1999; Gullick and LeChevallier, 2000; Johnson et al., 2000). Therefore, the likelihood for ethanol releases during transport, storage or mixing at blending terminals has increased (Powers et al., 2001a, b). This requires an improved understanding of the migration, fate and groundwater impacts of fuel-grade ethanol constituents following such releases. Particularly important are the lingering knowledge gaps about how the

*Corresponding author. Tel.: +1 713 348 3798; fax: +1 713 348 5239.
**Also corresponding author. Tel.: +1 713 348 5903; fax: +1 713 348 5203.
E-mail addresses: ncapiro@alumni.rice.edu (N.L. Cápiro), alvarez@rice.edu (P.J.J. Alvarez).

hygroscopic and buoyant properties of ethanol affect its behavior in unconfined aquifers (Rice et al., 1999a, b).

Highly concentrated ethanol may exert a cosolvent effect on hydrocarbons and enhance concentrations of benzene, toluene, ethylbenzene and xylenes (BTEX) in groundwater. This concern was addressed in recent groundwater modeling (Heermann and Powers, 1998; Powers et al., 2001a; Deeb et al., 2002; Molsen et al., 2002), laboratory (Rixey and He, 2001) and field (Rao et al., 1997; Ruiz-Aguilar et al., 2003) studies. Two-dimensional (2-D) tanks have also been employed to investigate the behavior of denatured (with 5% gasoline) ethanol and gasohol (gasoline with 10% v/v ethanol) spills in the absence of groundwater and capillary flow (McDowell et al., 2003; McDowell and Powers, 2003). In these 2-D gasohol studies it was shown that ethanol quickly partitions into vadose zone pore water and is initially retained above the water table (McDowell and Powers, 2003). This time-series photographic study detailed the potential for large volumes of highly concentrated ethanol to mobilize trapped light non-aqueous phase liquids (LNAPLs) (McDowell and Powers, 2003).

Bench-scale studies have also shown that highly concentrated fuel ethanol releases decrease surface and interfacial tensions, which reduces the height of the capillary fringe and results in a more compact and concentrated hydrocarbon contaminated zone (McDowell et al., 2003; McDowell and Powers, 2003). Ethanol (without hydrocarbons present) was also shown to migrate upwards into the capillary fringe and (at a retarded rate) move horizontally through it (Jawitz et al., 1998). Other researchers have verified the possibility of fluid migration in the capillary fringe (Silliman et al., 2002).

Despite the recent advances in our understanding of the potential behavior of fuel ethanol releases, previous studies have not quantitatively addressed the groundwater impacts of hydrocarbons associated with fuel ethanol over (representative) large spatial and temporal scales. Therefore, considerable uncertainty remains regarding the transport and potential groundwater impacts of ethanol releases at the field scale. To address these uncertainties and contribute to risk assessment, this paper reports on the behavior of fuel-grade ethanol injected in the subsurface of a near-field-scale, intensely monitored experimental release tank. The main objectives were to determine what hydrocarbons and ethanol concentrations can be expected in groundwater following spills of highly concentrated ethanol fuels (E95), characterize the disposition of LNAPL that is formed, and evaluate how long the ethanol source may last under conditions that are representative of field-scale releases (i.e., spill size, system dimensions, exposure duration, and groundwater depth). The large experimental system also permitted detailed groundwater measurements versus depth and length that contributed to the characterization of plume migration and mass balances, and the quantitative evaluation of impacts to groundwater quality.

2. Materials

2.1. Porous media

The experimental release tank system was packed with fine grain masonry sand obtained from Circle Sand (Houston, TX)

and the 2-D tank was filled with similar sand from US Silica (Ottawa, Illinois). The uniformity coefficients (D_{60}/D_{10}) based on sieve test particle size distribution (mm) for the masonry and Ottawa sand were 1.67 and 1.7, respectively. An average porosity of 0.31 was measured by with an earlier time-domain reflectometry (TDR), which falls into the typical range for sand (Freeze and Cherry, 1979). The sand was further characterized by the Texas A&M University Soil, Water and Forage Testing Laboratory (College Station, TX) with the following results: $f_{oc} = 0.0009$, pH = 6.8, 3 ppm of nitrate, 47 ppm of sulfur, and 31.31 ppm of bioavailable iron.

2.2. Fluids

A bromide tracer preceded the E95 release. This was made by dissolving crystalline sodium bromide (Fisher Scientific; Pittsburgh, PA) in tap water (151.4 L) to obtain the desired pulse concentration of 5000 mg L^{-1} over a 6 h injection period.

The E95 mixture contained 95% v/v 200 proof ethyl alcohol (AAPER Alcohol and Chemical Co., Shelbyville, KY) and 5% v/v NAPL mix composed of benzene (0.5% by weight), toluene (5.7%), m-xylene (11.9%), n-octane (52%), and tri-methyl benzene (TMB, 29.9%)—all purchased from Sigma Aldrich (Milwaukee, WI). Two dyes were added to the E95 mix. Fluorescein (Sigma Aldrich, CAS #: 2321-07-05), a hydrophilic dye, was added at 100 mg L^{-1} as a free acid and displayed a bright yellow color over a range of dilutions of Fluorescein-containing ethanol in water. Sudan-IV (Sigma Aldrich, CAS #: 85-83-6), a hydrophobic dye, was added at 100 mg L^{-1} to the NAPL and displayed a bright red color that indicated the presence of hydrocarbon. The NAPL mix, ethanol, and dyes were combined immediately prior to release into the experimental tank.

3. Methods

3.1. Bench-scale two-dimensional tank experiments

In preparation for the large-scale release, bench-scale experiments similar to those used elsewhere (Jawitz et al., 1998; McDowell et al., 2003; McDowell and Powers 2003) were conducted to observe the behavior of E95 injected at the water table in a continuous-flow system. The objectives of these experiments were to: (1) evaluate the potential for NAPL phase separation and formation of residual NAPL in the capillary fringe following release of E95, and (2) visualize the movement of the concentrated ethanol and NAPL that might occur in the large-scale experiments. The 2-D experiments were also used to help design of the near-field scale experiment, such as the selection of the E95 injection position, injection rate, and injection volume. These bench-scale experiments were different from previous 2-D studies which were not conducted under continuous flow conditions (McDowell et al., 2003) or with hydrocarbon NAPL (Jawitz et al., 1998).

These qualitative 2-D experiments were conducted in a continuous-flow glass-walled tank (30 cm × 30 cm × 1 cm) with a groundwater velocity of 0.1 cm min^{-1}. The system was packed with a coarse, light-colored sand mix from US

Silica (Ottawa, Illinois) to enhance visualization of the dyes, in a manner similar to that used to pack the large-scale tank (described below). A 20-mL injection of the NAPL mix containing $100\,mg\,L^{-1}$ Sudan-IV and $100\,mg\,L^{-1}$ Fluorescein was added at $2.4\,mL\,min^{-1}$.

3.2.   Pilot ethanol spill tank experiments

An 8150-L continuous-flow tank was used to conduct a quantitative ethanol release study. The purpose of this experiment was to characterize source zone generation and behavior, and to calculate mass balances in support of fate and transport assessments at the near-field scale. E95 (76 L) was spilled in the metal experimental tank, measuring $3.66\,m \times 1.83\,m \times 1.22\,m$ (Fig. 1). The average outdoor temperature ranged from 13 to 22 °C. The tank was open to the atmosphere and located outdoors under a canopy, and volatilization was not monitored. A $60\,cm \times 60\,cm$ window was installed in the middle of the tank to observe the behavior of contaminants at the injection point near the water table interface.

   The tank was packed with fine grain masonry sand (Circle Sand, Inc., Houston, TX) in 16 cm lifts using a front-end loader. Each lift was evenly spread using shovels and rakes followed by manual compaction using $30\,cm \times 30\,cm$ tampers. Concurrently, the tank was slowly filled with water from the bottom to minimize air pockets in the subsurface and stratification. After packing, the water level was raised above the sand surface to preclude the accumulation of trapped air. The water was then drained to the desired water table level of 0.74 m from base of tank with a vadose zone height of 0.4 m and an initial capillary fringe height of 0.25 m above the water table. This was a depth of approximately midway in the window, so that both the saturated and unsaturated zones could be observed.

   A continuous flow of tap water (pH of 7.53 ± 0.40 and ionic strength of 0.012–$0.006\,M\,L^{-1}$) was maintained in the tank through three inlet pipes within a screened well extending 30 cm below the water table. A steady flow rate of 800–$950\,mL\,min^{-1}$ was achieved by restricting flow out of the head driver on the system, a reservoir (1.8 m water depth), with a 1.27 cm ($\frac{1}{2}$ in) Swagelok ball valve. The outflow was consisted of three screened wells located 60 cm below the water table. The effluent was collected in a tank equipped with an overflow (at 60 cm above the base of the tank), before flowing to an activated carbon canister for treatment prior to discharge to the sewer system. The inlet reservoir tank coupled with the outlet overflow level maintained a hydraulic gradient of 0.03 ± 0.006 across the entire tank.

   Twenty-six sampling ports were initially installed downstream from the E95 injection wells or source zone, to monitor the passing groundwater plume. The sampling ports
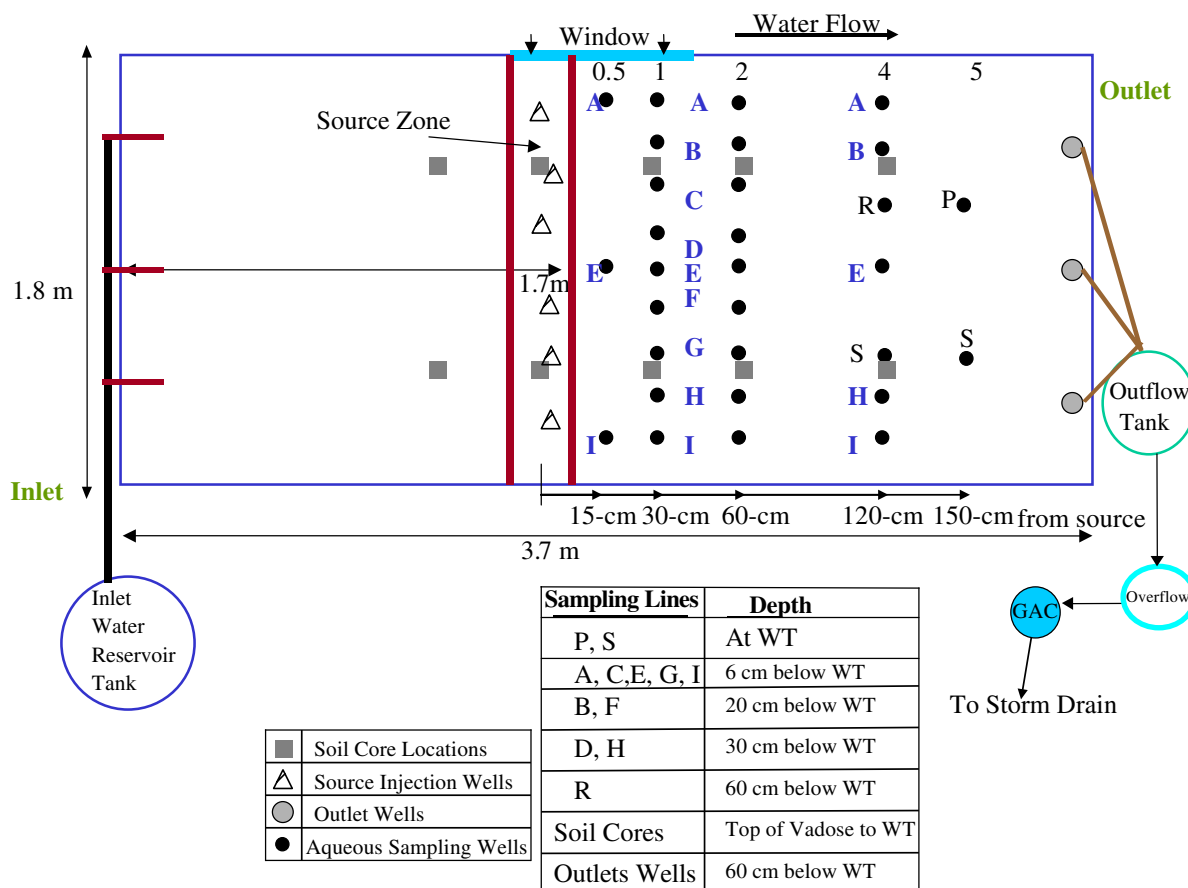

Fig. 1 – Plan view of experimental release pilot-scale tank and sampling well locations.

were located 15, 30, 60, and 120 cm (0.5, 1, 2, and 4 ft) down gradient from the source injection wells. At each distance, a port was placed on the centerline with four more ports equally spaced at 20 cm apart on either side. This created a line of 3 to 9 ports located at one of the five sampling depths below the water table: 1, 6, 20, and 30 cm, as shown in Fig. 1. After ethanol was released 4 additional ports were added at the down gradient end of our original sampling grid to assist in capturing the plume. A shallow line right at the water table (4S), and one deep line (4R) at the same depth as the outlet (60 cm below the water table) was added to the transect 120 cm (4 ft) away from the source, and a new final transect with two more shallow lines (5P and 5S) was added 150 cm (5 ft) away from the source, for a final total of 30 interior sampling locations (Fig. 1). Aqueous concentrations of bromide, NAPL mixture components and ethanol were monitored in the effluent to compare their migration patterns.

3.2.1. Hydraulic characterization

Several weeks prior to the addition of E95, a bromide tracer test was conducted to evaluate the hydraulic characteristics of the tank. A 151.4 L bromide pulse of 5000 mg L^{-1} was added through six injection ports at a flow rate of 70 mL (min-well)$^{-1}$ over a 6-h period. Aqueous samples (100 mL) were collected from the sampling ports in 125 mL HDPE field sampling bottles (Fisher Scientific; Pittsburgh, PA). Samples were collected every 1–2 h for the duration of the 1.5-day test.

Bromide concentrations were analyzed using a bromide ion selective electrode (Cole-Palmer). Analysis of the breakthrough curves estimated a seepage velocity ranging from 1.77 ± 0.44 m day^{-1} in the lines 20-cm below the water table to 3.45 ± 1.6 m day^{-1} in the shallow 6-cm lines. These values fall on the high end of typical reported groundwater velocities found in natural systems (Lovanh et al., 1999). The hydraulic conductivity was calculated to be $2.9 \pm 0.6 \times 10^{-2}$ cm s^{-1} in the medium-depth lines and $4.5 \pm 2.2 \times 10^{-2}$ cm s^{-1} in the shallow lines. The average hydraulic retention time over the length of the tank was about 3 days.

3.2.2. Source addition

Over a 3-h period, 76 L of fuel-grade ethanol was injected at the water table interface, at an average rate of 420 mL min^{-1} using six stainless-steel wells (70 mL (min-well)$^{-1}$). Acrylic walls were inserted down to the water table on either side of the source addition wells to fix the initial width of the spill and achieve conditions that would yield phase separation of NAPL near the point of injection. Preliminary experiments were conducted in the bench-scale cells by adding E95 incrementally until a free NAPL phase was observed. Using this same E95 to soil volumetric ratio, a source zone width was calculated that would achieve similar NAPL formation in the pilot tank. The acrylic walls were placed before the spill and were not removed after the injection to confine the source as it was injected. However, following complete injection, migration of ethanol and NAPL later occurred under the downstream wall and the E95 was subsequently able to migrate within the capillary zone. Six Masterflex pumps (Cole-Parmer; Vernon Hills, IL) using 0.635 cm ($\frac{1}{4}$ in) Viton tubing (Cole-Parmer; Vernon Hills, IL) were used to deliver E95 into the tank. The inlet end of the Viton tubing pulled pre-

mixed E95 from a feed container. The outlet end of each tube was connected by a hose clamp to a 60-cm segment of 0.635-cm ($\frac{1}{4}$ in) stainless-steel well inserted to the water table. The source injection ports were emplaced near the middle of the tank (adjacent to the observation window), and approximately 1.70 m from the inlet and 2.0 m from the outlet (Fig. 1).

3.3. Sampling procedures

Over 1000 aqueous samples and analyzed for ethanol, BTX, octane and TMB concentrations. Samples were collected in 40 mL glass vials, leaving no headspace, using 60 mL syringes (Fisher Scientific; Pittsburgh, PA). Prior to collecting each sample, each Viton tubing sample port was purged with 1.5 line volumes. The collection of samples occurred approximately every 3 h for the first 10 days, every 6 h for days 11–21, every 8 h for days 22–30, every 12 h for days 31–40, and once a day for the remaining 20 days of the experiment. The capped samples were stored at 20 °C until analysis was completed.

Sand cores were collected after ethanol and hydrocarbon concentrations in groundwater samples dropped below detection limits. The cores samples were taken from the sand surface to the water table (~40 cm) at five transects comprised of two equally spaced locations (~60 cm apart) including upstream, within, and downstream of the injection ports (Fig. 1). The cores were collected in 5 cm diameter HDPE cylinders, were sealed, and stored at 4 °C prior to analysis.

3.4. Analytical methods

Prior to analysis, groundwater samples were stored at 4 °C, followed by centrifugation at 2000 rpm for 5 min, and collection of supernatant into 2 mL gas-tight glass vials (Sun SRI; Duluth, GA). Aqueous samples were analyzed, as described elsewhere (He, 2002), by direct aqueous injection of 2 μL into a Hewlett Packard model 6890 gas chromatograph equipped with a Supelco (SPB-5) capillary column and a flame ionization detector (OI Analytical).

Sixty days following injection of E95, sand cores were collected and analyzed to assess the extent of NAPL distribution that had occurred. Sand samples were prepared by dividing each core ($L = 40$ cm, $r = 4.5$ cm) into three vertical segments and analyzing each segment for moisture content, ethanol, and BTX, TMB and octane concentrations (reported on a dry weight basis). Moisture (water+NAPL) content was determined by drying 10 g of soil in glass vials covered with aluminum foil at 200 °C for 8 h and measuring the loss of mass. To prepare the sand samples for ethanol and fuel component analysis, de-ionized water or HPLC-grade methanol, respectively, was added to 5 g of sand in a gas-tight 40 mL glass vial leaving no headspace. Each vial was then shaken vigorously for several minutes, placed on a vortex for 30 s followed by centrifugation at for 5 min. Following centrifugation, 4 mL of eluent was collected in a glass pipette and transferred to two 2 mL gas tight glass vials (Sun SRI; Duluth, GA) and stored at 4 °C until analysis by gas chromatography. Analyses for moisture content, ethanol and fuel components were done in duplicate.

Mass balances for bromide and E95 constituents were calculated by numerical integration of concentration vs. time

data. This calculation yielded a value of mass-time per unit volume for each effluent line (Liengme, 1997). This value was then multiplied by the corresponding average flow rate to calculate the effluent mass. The effluent and influent mass values were then compared for each constituent.

4. Results and discussion

4.1. 2-D bench-scale study

The 2-D bench-scale experiment corroborated previous work showing that ethanol migration is predominately confined to the capillary zone even when injected at or below the water table (Jawitz et al., 1998), and provided a pictorial documentation of the movement of the concentrated ethanol and NAPL that might occur in the large-scale experiment (Fig. 2). Specifically, the series of photographs show: (1) the E95 injection at the water table (1 min); (2) upon injection the E95 moves vertically upwards due to buoyancy and interfacial tension gradient driven flow, and also laterally with the flow of pore water in the capillary fringe (12 min); (3) NAPL phase separates from E95 as it mixes with water in the capillary fringe (40 min); and (4) after five pore volumes of elution, some of the fluorescein-stained ethanol remains in the capillary fringe (48 h). Residual (Sudan IV-stained) NAPL is

also left behind. A significant reduction in capillary height due to lower surface tension was also observed, as reported by others (McDowell et al., 2003). This shows that some ethanol remained in the pore water. A 50% reduction in capillary height would correspond to a surface tension of $36\,\mathrm{dyn\,cm^{-1}}$ which would indicate an ethanol aqueous concentration of approx. 30 vol% (Weast and Astle, 1981).

Although it is not surprising that E95 (which has lower density than water) moved upward into the capillary fringe, it should be pointed out that the same volume of a lighter 100% hydrocarbon NAPL (density $= 0.77\,\mathrm{g\,cm^{-3}}$ versus $0.79\,\mathrm{g\,cm^{-3}}$ for E95) did not rise into the capillary fringe when injected into the same system (pictures not shown). Rather, a NAPL pooled at the water table. Apparently, differences in interfacial tension and miscibility influenced the different behavior for E95 versus the pure hydrocarbon NAPL.

4.2. Plume migration in pilot-scale tank

The large-scale spill exhibited similar migration patterns to those observed in the 2-D bench-scale experiment, with E95 transport primarily constrained to the pore water above the water table and at the water table interface. Nearly all of the 1000+ samples analyzed from the 26 original sampling ports (located at depths 6–30 cm) over the 60-day experiment had
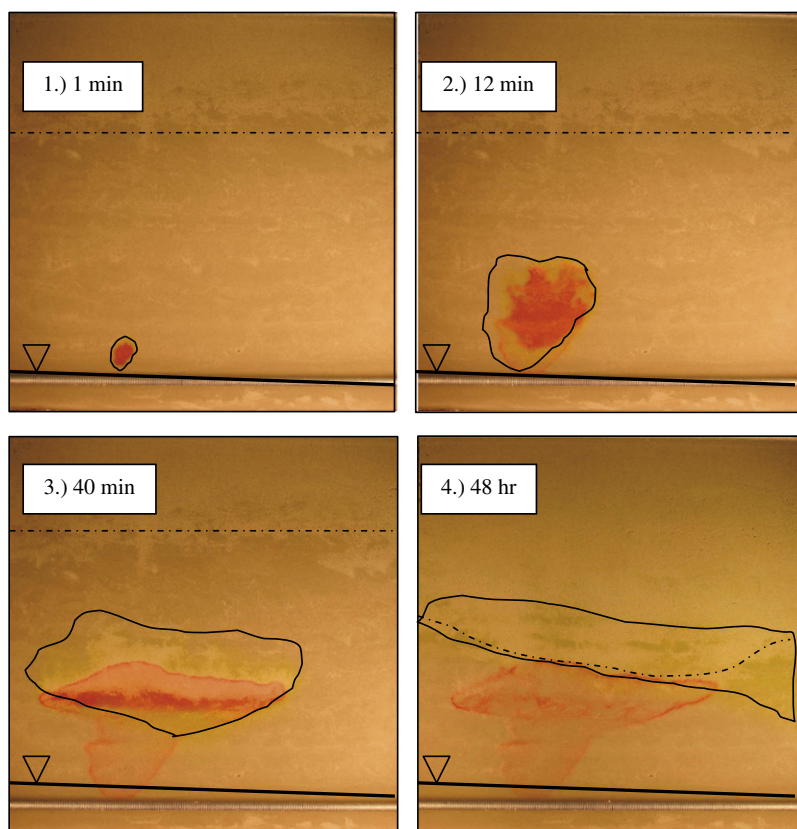

Fig. 2 – Bench-scale visualization of E95 (containing Sudan IV and fluorescein dyes) released at the water table in a 2-D tank. Time after injection is depicted. Injection volume $= 20\,\mathrm{mL}$ at $2.4\,\mathrm{mL\,min^{-1}}$. Solid line represents outer contour of fluorescein dye; dotted line represents top of capillary fringe.

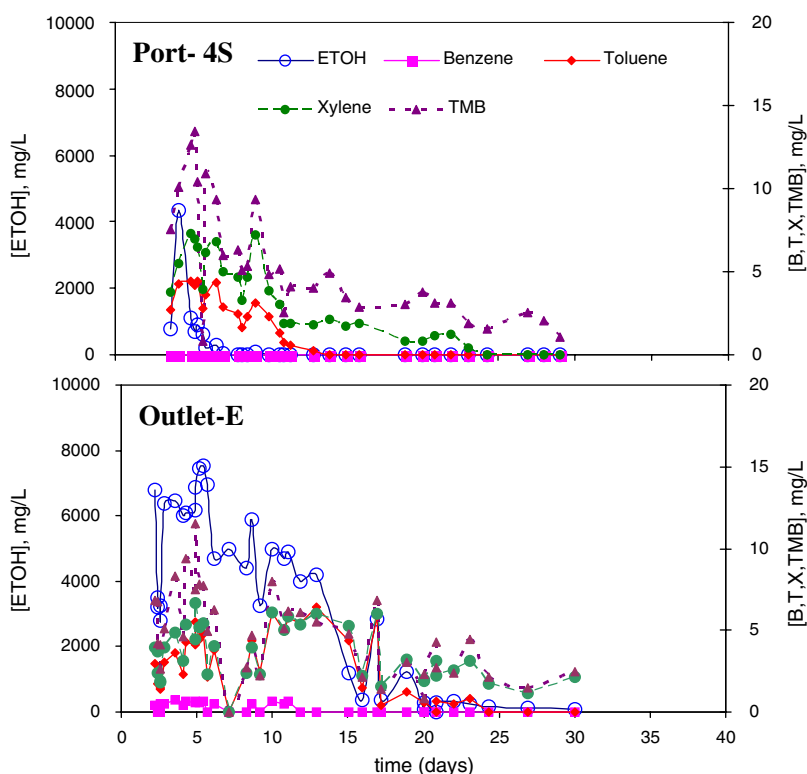| Table 1 – Aqueous ethanol concentrations measured over 30 days		
Line location	Avg. concentration (mg L^{-1})	Max. concentration (mg L^{-1})
6–30 cm below WT	<1	10
Just below WT	2000	7000
Outlet A	4000	9600
Outlet E	4000	7500
Outlet I	4000	7500

Fig. 3 – Representative ethanol and hydrocarbon breakthrough curves at two locations. Line 4S is at the water table, and outlet E is the average passing through the center of the tank (pulled down from the capillary fringe) (see Fig. 1).

no detectable concentrations of ethanol (Table 1). However, fluorescein dye was visible in the effluent 3 days after ethanol was released. This indicated that ethanol traveled the length of the tank at or above the water table, thus evading the groundwater sampling ports. Therefore, three new shallower sampling ports were installed at the water table at 120 cm and 150 cm downstream of the source injection ports (4S, 5S, and 5P, Fig. 1). Samples from these new ports yielded higher ethanol concentrations, near 7000 mg L^{-1} with an average of 2000 mg L^{-1} over 20 days. Analysis of effluent samples showed peak ethanol concentrations of nearly 10,000 mg L^{-1}, with a 30-day average of 6000 mg L^{-1} (Table 1 and Fig. 3).

4.2.1. Comparison to bromide tracer migration

Whereas ethanol migrated at the water table interface or through the high water-saturation regions of the capillary zone (Fig. 4(A)), the bromide tracer migrated through the saturated zone and was detected in all of the shallow

(6 cm below water table) and middle depth lines (20 cm below water table) near the outlet (Fig. 4(B)). Compared to bromide, ethanol moved 10 times slower (at 0.3±0.04 m day^{-1}) (Fig. 5), despite being injected at the same location and rate under the same tank flow conditions. Apparently, ethanol partitioning into vadose-zone pore water (due to its hygroscopic and buoyant properties) retarded its horizontal migration and restricted its vertical dispersion through the saturated zone.

4.2.2. Fuel-grade ethanol aqueous recovery

Analysis of effluent samples yielded a 98% recovery for ethanol (Fig. 5), which was much higher than the corresponding values for of the monitored hydrocarbons (i.e., 22% for benzene, 36% for toluene, 0% for octane, 28% for *m*-xylene, and 14% for trimethylbenzene). These lower hydrocarbons recoveries were likely due to hydrocarbon retention as residual NAPL following E95 phase separation in the capillary
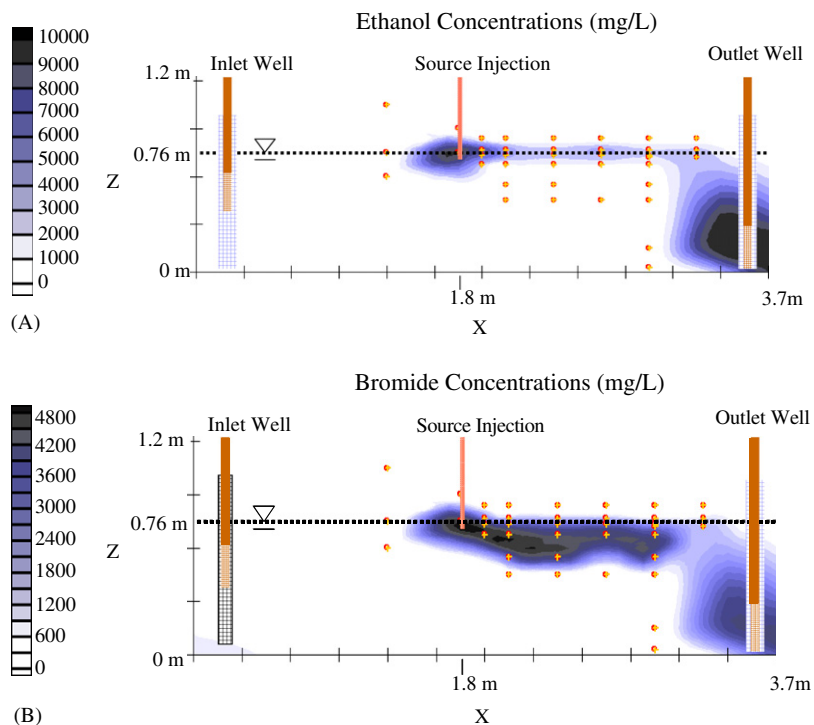
Fig. 4 – Vertical cross-section interpolations (calculated using constant natural neighbors methods) showing maximum concentrations found at sampling locations: (A) ethanol plume transport, and (B) bromide tracer transport. *Note*: Migration pathways near outlets caused by plume reaching the end of the tank and being drawn down by effluent wells.
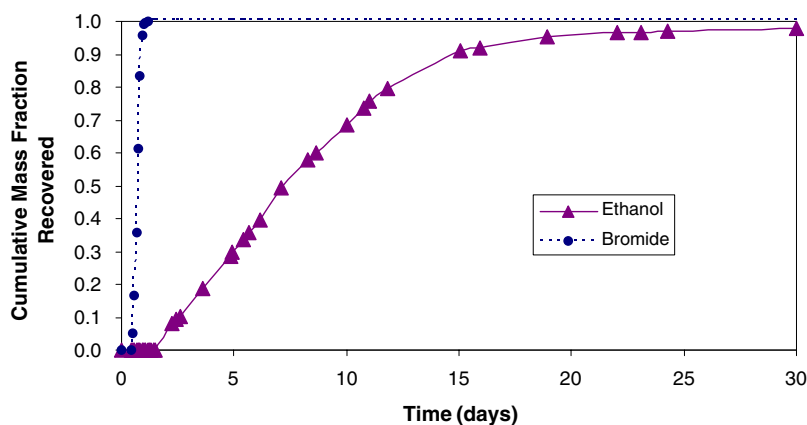

Fig. 5 – Cumulative ethanol and bromide mass recovered from three outlets vs. time normalized to mass added at source.

fringe, and possibly also due to volatilization, sorption and biodegradation losses that were not quantified.

The high recovery for ethanol in the effluent indicates that losses due to volatilization of ethanol were not significant as suggested by other research (Dakhel et al., 2003). This is due to the high solubility and low volatility of ethanol from water (dimensionless Henry's constant of 0.000252 at 25 °C, the upper temperature range during experiment). Significant ethanol biodegradation losses were unlikely in this system due to the formation of a thin layer of ethanol with relatively high ($>10,000 \, \text{mg L}^{-1}$) and possibly toxic concentrations

(Powers et al., 2001a). The lack of significant biodegradation was corroborated by the absence of detectable byproducts, such as acetate (Da Silva and Alvarez, 2002).

4.3.   Distribution of ethanol and BTX compounds

The ethanol–NAPL mix migrated laterally above the water table both up gradient and down gradient of the injection ports (Fig. 4(A)). This co-transport of hydrocarbons with ethanol through the capillary fringe suggests the possibility of source zone migration towards potential receptors.

Evidence of such source zone migration was initially provided by observations of Sudan-IV red stains (associated with hydrocarbons) on vertical PVC pipes installed to monitor water levels both up gradient and down gradient of the source zone. The stains occurred only upwards from the water table level into the capillary fringe. Analogous to the 2-D visualization study, vertical migration of the LNAPL upwards from the water table into the capillary zone was observed in the large-scale tank window (Fig. 6). The window also allowed for visualization of the capillary zone height reduction (by ~30–40%) following the introduction of E95.

4.4. Soil sample results

Soil core data (Table 2) taken at the end of the experiment (after 60 days) provided further evidence that the bulk flow of E95 was restricted to the high water saturation regions of the capillary fringe. The soil results support the high recovery of ethanol calculated in the aqueous mass balance, because ethanol was not detected in the five vadose zone transects. The cores also provided evidence of BTX, TMB and octane remaining in the soil as indicated by the presence of Sudan-IV red and a strong hydrocarbon odor. Apparently, ethanol and hydrocarbons migrated down gradient together in the capillary fringe until ethanol was diluted by pore water to a point that diminished its cosolvent effect, and this promoted the separation of the hydrocarbons phase, which is also supported by observations from the 2-D visualization study. This left a residual NAPL lens that expended at least 1.3 m downstream of the source that in part accounts for the poor recovery of hydrocarbons in the aqueous effluent samples.
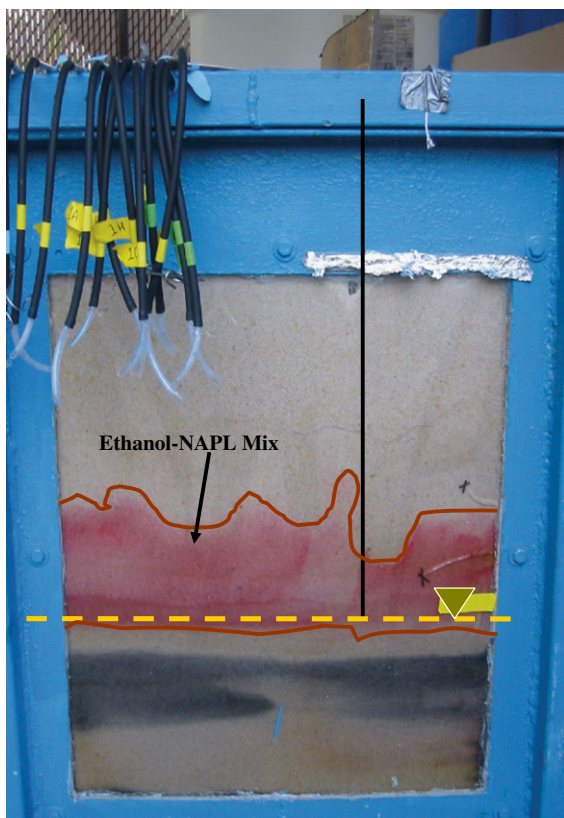

Fig. 6 – Picture of window on the side of tank showing NAPL (Sudan IV) staining of the sand above the water table (dashed line). The vertical line represents one of the acrylic walls that were inserted on either side of the source injection location. Note: **The black area was present prior to E95 addition and is likely attributed to phototrophic microbial growth, since it was only found at the window.**

5. Conclusions and implications

When spilled at the water table interface, fuel ethanol is likely to migrate upwards and spread laterally within the high water content regions above the water table. Once in the capillary fringe, ethanol is likely to migrate down gradient at a slower rate than constituents in the saturated zone, but at a rate that may still lead to relatively rapid depletion of ethanol from the source of the spill. Furthermore, the 5% v/v hydrocarbons added as a denaturant to E95 are likely to undergo phase separation and form a residual LNAPL in the capillary fringe. The migration of ethanol and the formation of LNAPL will be mainly confined to the capillary zone, resulting in ethanol and hydrocarbon impacts to groundwater near the source that are likely to be lower than expected by only considering ethanol's complete miscibility with water. The

Table 2 – Maximum concentrations found at any depth in capillary zone cores collected 60 days after the E95 release (reported on a dry weight basis)				
Compound	30 cm upstream of injected source (mg kg^{-1})	30 cm downstream of injected source (mg kg^{-1})	60 cm downstream of injected source (mg kg^{-1})	120 cm downstream of injected source (mg kg^{-1})
Ethanol	<1	<1	<1	<1
Benzene	35	37	19	28
Toluene	39	47	28	25
m-Xylene	157	152	66	49
1,2,4-Tri-methyl benzene	850	726	154	273
n-Octane	351	355	300	226

buoyancy and interfacial tension gradient driven flow of ethanol through the capillary zone is also likely to confound down gradient ethanol and hydrocarbon concentrations in groundwater. Therefore, characterization of sites contaminated with fuel-ethanol is likely to be more difficult than sites contaminated by hydrocarbons alone. Potential changes in capillary fringe height due to an ethanol-induced reduction in surface tension and mixing effects due to water table fluctuations would add further complexity to the determination of the rate of contaminant drainage into groundwater and LNAPL volume trapped in the vadose zone.

Acknowledgments

R E F E R E N C E S

BRP, 1999. Achieving Clean Air and Clean Water: The Report of the Blue Ribbon Panel on Oxygenates in Gasoline. EPA420-R-99-021, Washington, DC.

Dakhel, N., Pasteris, G., Werner, D., Hohener, P., 2003. Small-volume releases of gasoline in the vadose zone: impact of the additives MTBE and ethanol on groundwater quality. Environ. Sci. Technol. 37, 2127–2133.

Da Silva, M.L., Alvarez, P.J.J., 2002. Effects of ethanol versus MTBE on benzene, toluene, ethylbenzene, and xylene natural attenuation in aquifer columns. ASCE J. Environ. Eng. 128, 862–867.

Deeb, R.A., Sharp, J.O., Stocking, A., McDonald, S., West, K.A., Laugier, M., Alvarez, P.J.J., Kavanaugh, M.C., Alvarez-Cohen, L., 2002. Impact of ethanol on benzene plume lengths: microbial and modeling studies. ASCE J. Environ. Eng. 128, 868–875.

Gullick, R.W., LeChevallier, M.W., 2000. Occurrence of MBTE in drinking water sources. J. Am. Water Works Assoc. 92, 100–113.

He, X., 2002. Ethanol-enhanced dissolution of aromatic hydrocarbons from non-aqueous phase liquids in porous media. Ph.D Thesis, University of Houston, Houston, TX.

Heermann, S.E., Powers, S.E., 1998. Modeling the partitioning of BTEX in water-reformulated gasoline systems containing ethanol. J. Contam. Hydrol. 34, 315–341.

Jawitz, J.W., Annable, M.D., Rao, P.S.C., 1998. Miscible fluid displacement stability in unconfined porous media: two-demensional flow experiments and simulations. J. Contam. Hydrol. 31, 211–230.

Johnson, R., Pankow, D., Bender, C.P., Zogorski, J., 2000. MTBE—to what extent will past releases contaminate community water supply wells? Environ. Sci. Technol. 34, 210A–217A.

Liengme, B.V., 1997. A Guide to Microsoft Excel for Sceintific and Engineers. Wiley, New York, NY, pp. 146–162.

Lovanh, N., Zhang, Y.-K., Alvarez, P.J.J., 1999. Statistics and effect of first-order biodegradation rate coefficient on intrinsic remediation of groundwater contamination. In: Sixth International Petroleum Environmental Conference, Houston, TX.

McDowell, C.J., Powers, S.E., 2003. Mechanisms affecting the infiltration and distribution of ethanol-blended gasoline in the vadose zone. Environ. Sci. Technol. 37, 1803–1810.

McDowell, C.J., Busheck, T., Powers, S.E., 2003. Behavior of gasoline pools following a denatured ethanol spill. Ground Water 41, 746–757.

Molsen, J.W., Barker, J.F., Frind, E.O., Schirmer, M., 2002. Modeling the impact of ethanol on the persistence of benzene in gasoline-contaminated groundwater. Water Resources Res. 38 (4–1), 4–12.

Powers, S.E., Hunt, C.S., Heermann, S.E., Corseuil, H.X., Rice, D., Alvarez, P.J.J., 2001a. The transport and fate of ethanol and BTEX in groundwater contaminated by gasohol. Crit. Rev. Environ. Sci. Technol. 31, 79–123.

Powers, S.E., Rice, D., Dooher, B., Alvarez, P.J.J., 2001b. Will ethanol-blended gasoline affect groundwater quality? Environ. Sci. Technol. News 35, 24A–30A.

Rao, P.S.C., Annable, M.D., Sillan, R.K., Dai, D., Hatfield, K., Graham, W.D., 1997. Field-scale evaluation of in situ cosolvent flushing or enhanced aquifer remediation. Water Resources Res. 33, 2673–2686.

Rice, D.W., Alvarez, P.J.J., Powers, S.E., Beller, H., Kane, S., Layton, D.W., Daniels, J.I., Dooher, B., 1999a. Knowledge gaps regarding the surface water and groundwater impacts of ethanol-containing gasoline and recommendations for future research. UCRL-AR-135949. State of California, Sacramento.

Rice, D.W., Powers, S.E., Alvarez, P.J.J., 1999b. Potential scenarios for ethanol-containing gasoline released into surface and subsurface waters. UCRL-AR-135949. State of California, Sacramento.

Rixey, W.G., He, X., 2001. Dissolution characteristics of ethanol from NAPL sources and the impact on BTX groundwater concentrations. In: Conference on Petroleum Hydrocarbons and Organic Chemicals in Groundwater. Ground Water Publishing Company, Houston, TX, pp. 41–52.

Ruiz-Aguilar, G.M.L., O'Reilly, K., Alvarez, P.J.J., 2003. A comparison of benzene and toluene plume lengths for sites contaminated with regular vs. ethanol-amended gasoline. Ground Water Remediation 22, 1–6.

Silliman, S.E., Berkowitz, B., Simunek, J., van Genuchten, M.T., 2002. Fluid flow and solute migration within the capillary fringe. Ground Water 40, 76–84.

Weast, R.C., Astle, M.J. (Ed.), 1981. CRC Handbook of Chemistry and Physics, 62nd ed. CRC Press, Inc., Boca Raton, FL.

Zogorski, J.S., Morduchowitz, A., Baehr, A. L., Bauman, B. J., Conrad, D. L., Drew, R. T., Korte, N. E., Lapham, W. W., Pankow, J. F., Washington, E. R., 1996. Fuel Oxygenates and Water Quality—Current Understanding of sources, Occurrence in Natural Waters, Environmental Behavior, Fate and Significance—Final Report. Office of Science and Technology Policy, Executive Office of the President, Washington, DC.